Proceedings of ASME 28th International Conference on Ocean, Offshore and Arctic Engineering
OMAE2009
May 31- June 5, 2009, Honolulu, Hawaii

OMAE2009-79960

NUMERICAL INVESTIGATION OF THE FLOW THROUGH AND AROUND A NET CAGE

Kyujin Shim
Fisheries and Aquaculture
SINTEF
Trondheim, Norway
Kyujin.Shim@sintef.no

Pascal Klebert
Fisheries and Aquaculture
SINTEF
Trondheim, Norway
Pascal.Klebert@sintef.no

Arne Fredheim
Fisheries and Aquaculture
SINTEF
Trondheim, Norway
Arne.Fredheim@sintef.no

ABSTRACT

Structure and design of fish cages can be improved by the knowledge of the flow pattern around and inside the net cages. To address this problem, commercially available computational fluid dynamics (CFD) software is used to analyze this problem by calculating the drag and the flow velocity distribution around cylinders with different porosities. The results of these simulations are compared with the data from experiments which have been previously published. Aquaculture cages are very large structures that consist mainly of netting, which can be approximated by small cylinders connected at knots. But due to the large number of these cylinders (millions for a single salmon farming cage), it is computationally expensive to model the exact geometry. Bio fouling is another factor which is of particular interest as fouled nets(lower porosity) can significantly reduce flow of well-oxygenated water reaching the fish during normal rearing conditions. Therefore the numerical approach used to simulate the flow through and around the net cage is to consider it as a circular cylinder with a porous jump boundary. Drag coefficient and flow pattern are compared with available experimental data. Vertical cylinders are used for this study. Different porosities have been used for the simulations as for the experiments (0%, 75%, 82% and 90% open area) in order to simulate the impact of the fouling on the load of the net structures and the flushing of the cage. The results show that a porous jump with a pressure drop proportional to velocity squared has the best agreement with measured data.

Keywords: Fish cages; porous jump boundary; CFD; drag coefficient; velocity defect

NOMENCLATURE

A	projected area of the cylinder
a	inertia loss
b	viscous loss
Bl	blockage
C_2	pressure-jump coefficient
C_D	drag coefficient
D	diameter of cylinder
F_D	drag force
L	length of cylinder
Δm	thickness of the medium
Δp	pressure drop
P	static pressure
Re	Reynolds number = $\frac{\rho v A}{\mu}$
Y^+	Non-dimensional cell distance from wall
α	face permeability
μ	fluid viscosity
v	Towing speed
ρ	density of fluid

INTRODUCTION

CFD(Computational Fluid Dynamics) has been applied to fluid flow problems on various industrial applications. Until recently, the development of CFD technology and high performance of computers provide the possibility to deal with complex flow by highly accurate numerical simulation along with experiments. Especially, a simulation of flow past a circular cylinder has been focused on Strouhal number, drag and lifts coefficients and developed by many researchers. Because circular cylinder is important part of structure analysis and engineering and it has been applied to many practical applications, e.g bridge piers, periscope, towers, masts, cables

and wire. And the knowledge about various load of flow dynamic structure for hydrodynamic and aerodynamic is crucial for design and control. Most of studies on circular cylinders are related to solid cylinders, cylinders oscillation, wall mounted cylinder and cylinders near the wall.

Recently, a study of fish cages has been investigated by using of finite element method. This method makes it possible to predict the dynamic behavior of fish cages which are affected by internal and external forces. (Tsukrov, 2003). And the simulation(Lader and Fredheim, 2006) of a single net sheet exposed to waves and current was conducted with super-elements approach and the dynamic properties of such an elastic structure were investigated. Huang(2008) suggested suitable model to analyze the maximum tension on the mooring lines and its corresponding volume reduction coefficient due to the combination effect of waves and currents on a net-cage system. The author used numerical algorithm with Morison equation to calculate the wave forces acting on small components of the cage structure. These kinds of studies can calculate the dynamic behaviour of structures with environmental such as waves and currents. But it can not predict the flow pattern inside and in the wake of the fish cages. A better knowledge about the flow field through and around Marine net panels will help to establish better models for the prediction of the distribution of dissolved nutrients, oxygen and particles in and around net panels.

CFD with FVM (finite volume methods) needs CPU time and data space when a net panel represent through an actual configuration. But if the net panel will simulate with simple boundary condition, it can be simulate with less CPU times and less data spaces.

This study presents a drag coefficient comparison between CFD simulation and tests on a series of cylinders with varying porosity. The experiments were carried out in a towing tank and PIV (Particle Image Velocimetry) has been used to the velocity field. The experiment results(Gansel et al.,2008) of vertical solid cylinder and porous cylinder were compared.

NUMERICAL SIMULATION

Numerical simulations have been performed for towing tested in water channel for vertical solid cylinder, 75%, 82% and 90% open cylinder at 0.05 and 0.2 m/s inlet velocity. In this study, FLUENT a commercial CFD program is used for the simulation. It is based on Finite Volume Method. The fluid dynamics for Analysis of fish cages with porous boundary condition basically consists with continuity equation and momentum conservation equations. Incompressible flow is used for these steady state simulations and turbulence is modelled by using the realizable k-ε model. SIMPLE(Semi-Implicit Method for Pressure-Linked Equations) algorithm used for pressure–velocity coupling . A first order upwind scheme is used for discretization. Maximum residual tolerance was set under the 1×10^{-6}.

Fig. 1 shows the geometry for a 3D simulation of vertical cylinder. Turbulent conditions at inlet have been considered with low level of turbulent intensity due to the towing tank experiment condition. A rectangular domain is used to simulate the flow around a fixed cylinder. The boundary conditions are imposed in such a way that the flow is from the left toward the right of the domain. A circular cylinder is placed inside the domain with its center being 15D away from the inlet and 35D away from the outlet. The domain has a transverse dimension of 6D. These dimensions have 2.5D from cylinder to sidewall, might be introduce the boundary wall effects. The width of the channel was 6D and the height 10D introducing a blockage of *Bl*=5%.

Fig. 2 shows grid system for solid and porous cylinder. Mixed(hexahedral and tetrahedral) cells model was used for numerical simulation which is chosen after a grid dependency test. Optimization of the computational domain carried out with various interval points at the circumference of the circular cylinder. The first cells normal to the cylinder surface along the circumference of circular cylinder are fixed from $Y^+ \approx 1$ to which is reasonable enough to model the near wall effect. Since the Fluent does not have a function for plotting drag force on a porous boundary area, the forces on the porous jump surface have to be found using some other method: a force balance over the control volume of the channel is used in this case but it requires a proper wall force resolution. For that reason, the density of the grid is higher on side and bottom walls.

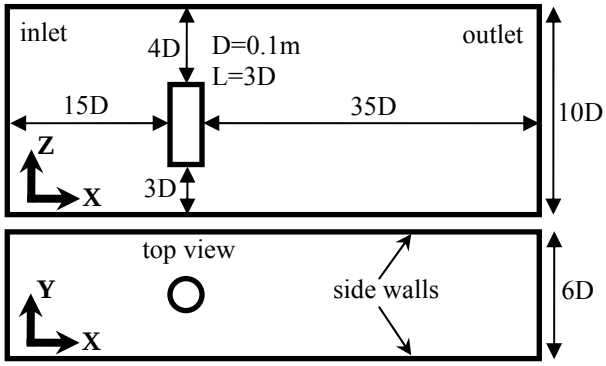

Fig.1. Geometry of finite cylinder for 3D simulation. Top: Cross-sectional view in ZX plane. Bottom: Cross-sectional view in XY plane.

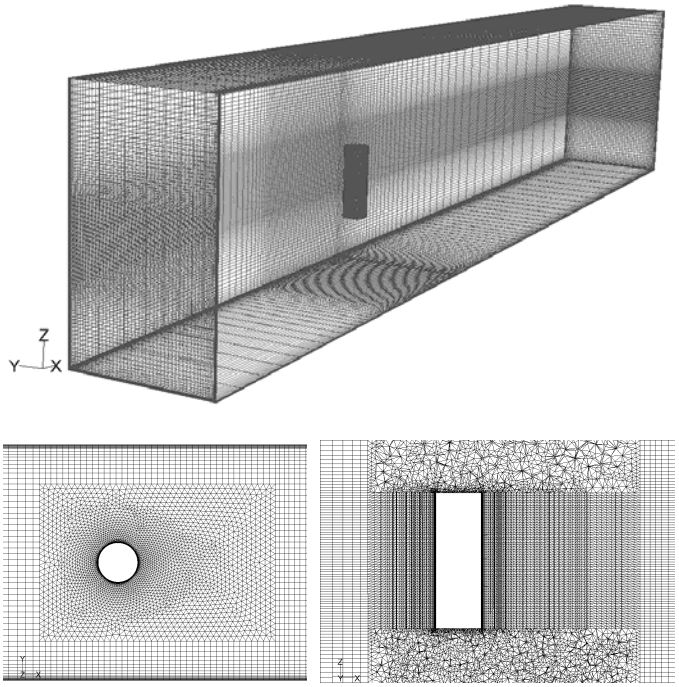

Fig.2. 3D view of the complete grid(top), sectional view in XY plane(left) and sectional view in XZ plane(right)

BOUNDARY CONDITION

In order to simulate the porosity of a net cage the porous jump boundary condition available in FLUENT package was used: this condition can be used for modeling a wide variety of engineering applications, including flows through packed beds, filters, perforated plates, flow distributors and tube banks. It is generally desirable to determine the pressure drop across the porous area and to predict the flow field in order to optimize a given design. Porous jump conditions are used to model a thin membrane that has known velocity (pressure-drop) characteristics. This simple model has been used instead of the full porous media model also available, because of its robustness and better convergence. Porous jump boundary condition applies a pressure drop across a boundary that can be described by

$$\Delta p = \left(\frac{\mu}{\alpha} v + C_2 \frac{1}{2} \rho v^2 \right) \Delta m \qquad (1)$$

The measured drag force on the porous cylinder and current through the porous cylinder related with towing speed can be used to calculate a and b by least squares method. Then the face permeability and pressure-jump coefficients were calculated from a and b. Pressure drop consists of two terms, an inertia loss and viscous loss :

$$\Delta p = a \cdot v^2 + b \cdot v$$

$$a = \frac{1}{2} \rho C_2 \Delta m \,, \qquad b = \frac{\mu \Delta m}{\alpha} \qquad (2)$$

where a is inertia loss term, b is viscous loss term. Fig 3 shows the least squares method curve fit between the towing speed and the pressure drop on a porous cylinder.

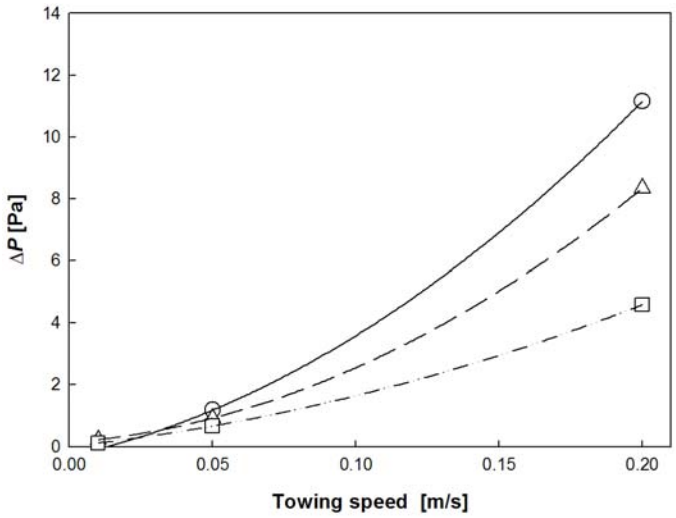

Fig. 3. Least squares method curve fit between towing speed and pressure drop on a porous cylinder from experiment of Gansel et al.(2008). ○ 75%, △82% and □ 90% open cylinders, respectively.

Table 1 Face permeability and pressure-jump coefficient for the porous cylinder

Open area [%]	75	82	90
Face permeability	8.77×10^{-8}	8.85×10^{-8}	9.9×10^{-8}
Pressure-jump coefficient	444	304	128

RESULTS

Suitable for CFD simulations with porous body, the porous jump conditions is investigated and applied to flow analysis on fish cages. The drag on a porous surface is calculated from the momentum balance. The FLUENT provides as output the pressure and velocity fields on the computational domain. The momentum balance on a control volume around the porous cylinder carried out the net force on the body as a function of the change in momentum of the fluid passing through the cont-

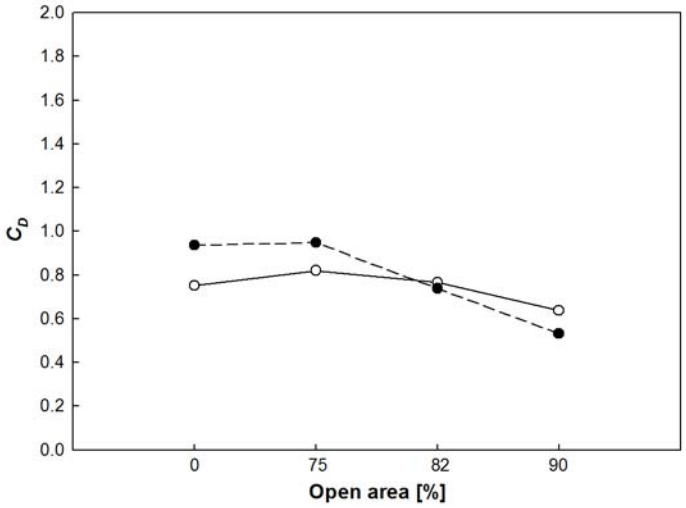

Fig. 4. Drag coefficient comparison with experiment and simulation for 0%, 75%, 82% and 90% open cylinder at Re=5000. ○: experiment(Gansel et al.,2008) ●: simulation.

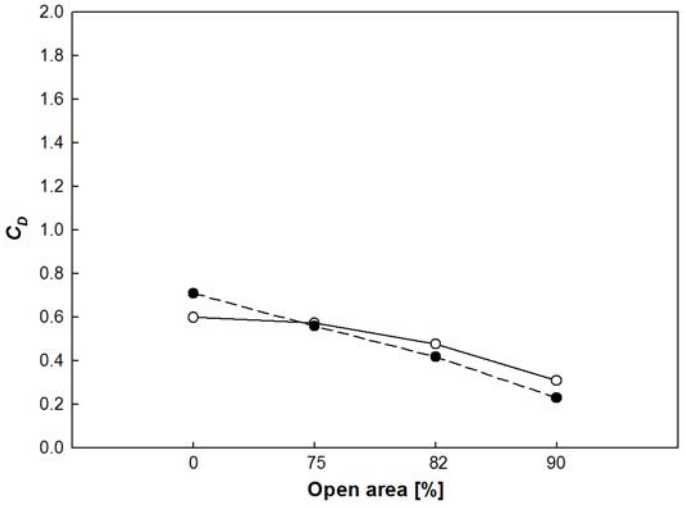

Fig. 5. Drag coefficient comparison with experiment and simulation for 0%, 75%, 82% and 90% open cylinder at Re=20000. ○: experiment(Gansel et al.,2008) ●: simulation.

rol volume and the net pressure force on the control volume. For the net force in the *i*th direction, this momentum balance is:

$$F_i = \int_{cs} P dA_i - \int_{cs} \rho v_i v \cdot dA \tag{3}$$

where PdA_i represents the component of the pressure force acting in the *i*th direction. The drag force is defined as the force acting opposite to the flow direction, the drag coefficient on the porous cylinder can be described by

$$C_D = \frac{F_D}{1/2 \cdot \rho \cdot A \cdot v^2} \tag{4}$$

Fig 4 and Fig. 5 shows comparison between simulation and experiment of drag coefficient by Gansel et al.(2008). The simulation results are very dependent on the turbulent model used. The present simulation uses the realizable k-ε model. The drag coefficient decreases with the increasing porosity of the porous models for Re=5000 and Re=20000. The cylinder with a high open area allows the fluid to flow through it with the least resistance, hence the drag must approach zero for the high porosity case. Whereas, a porous cylinder with very low open area will allow little fluid to pass through it. The drag coefficient of 0% open cylinder for Re=20000 better match between experiment and simulation than Re=5000. The difference in drag coefficient from 0% open to the 75% open cylinder is only 2% for Re=5000 and 26% for Re=20000 for the experiment results of Gansel et al.(2008) while the simulation shows 8% for Re=5000 and 6% for Re=20000. The decrease of the drag with porosity from the 75% to the 90% open cylinder is 43% for Re=5000 and 58% for Re=20000 for experiment results of Gansel et al.(2008) while the simulations show 22% for Re=5000 and 45% for Re=20000. 82% open cylinder at Re=5000 and 75% open cylinder at Re=20000 show most reasonable agreement for drag coefficient results.

Fig. 6 and 7 shows comparison of velocity defect between experimental data and the present simulation in the wake of solid and porous cylinders at 1.5 diameter downstream from the centerline of the cylinder for Re=5000 and Re=20000. The numerical results show smooth pattern. Specially, the simulation with 75% and 82% open cylinders are similar when compared to the experiments results. But the comparison between experiment and simulation for the 90% open cylinder is not good, because of the fluctuations of the experiment velocity due to the individual wakes generated by the single strings of the net within $-0.5 < y/d < 0.5$ (both for Re=5000 and Re=20000) as stated by Gansel et al.,2008: this effect can't be reproduced by the porous jump feature used in the simulation. At 0% open cylinder, the velocity profile of the simulation shows a more narrow area than the experiment: within $-0.36 < y/d < 0.36$ for Re=5000 and $-0.28 < y/d < 0.28$ for Re=20000 and $-0.54 < y/d < 0.53$ for Re=5000 and $-0.50 < y/d < 0.57$ for Re=20000. The hollow area on top position of 0% open cylinder suggested recirculation area at the simulation as can be seen Fig. 8a. As a result of the cylinder's blockage effect, water is accelerate in flow direction. This leads to negative velocity defect on the side of cylinder for $y/D < -1.0$ and $y/D > 0.9$ at Fig. 6a and Fig. 7a.

The streamlines through the increase open area are presented in Figs. 8a-d for Re=5000. For a 0% open cylinder, the vorticity diffuses from the surface into the external flow field, whereas, for the porous cylinder vorticity diffuses into

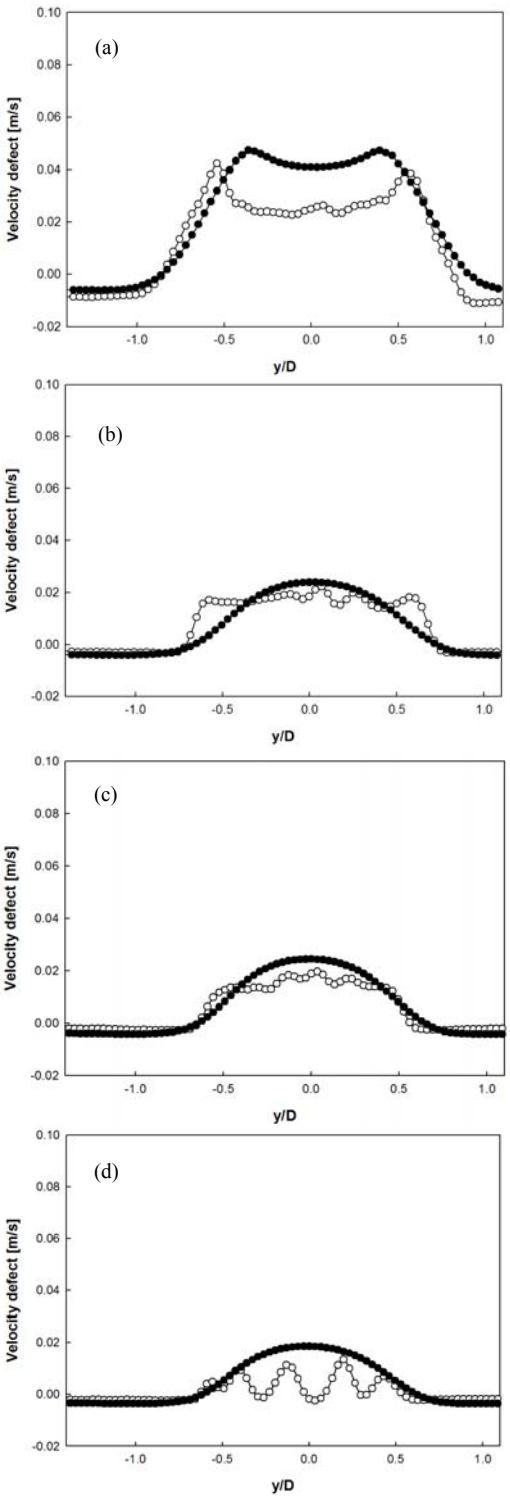

Fig.6. Velocity defect comparison with experiment and simulation in the wake of 1.5 diameter downstream from the centerline of the vertical cylinder at Re=5000. (a) 0% open cylinder; (b) 75% open cylinder; (c) 82% open cylinder; (d) 90% open cylinder. ○: experiment(Gansel et al.,2008) ●: simulation.

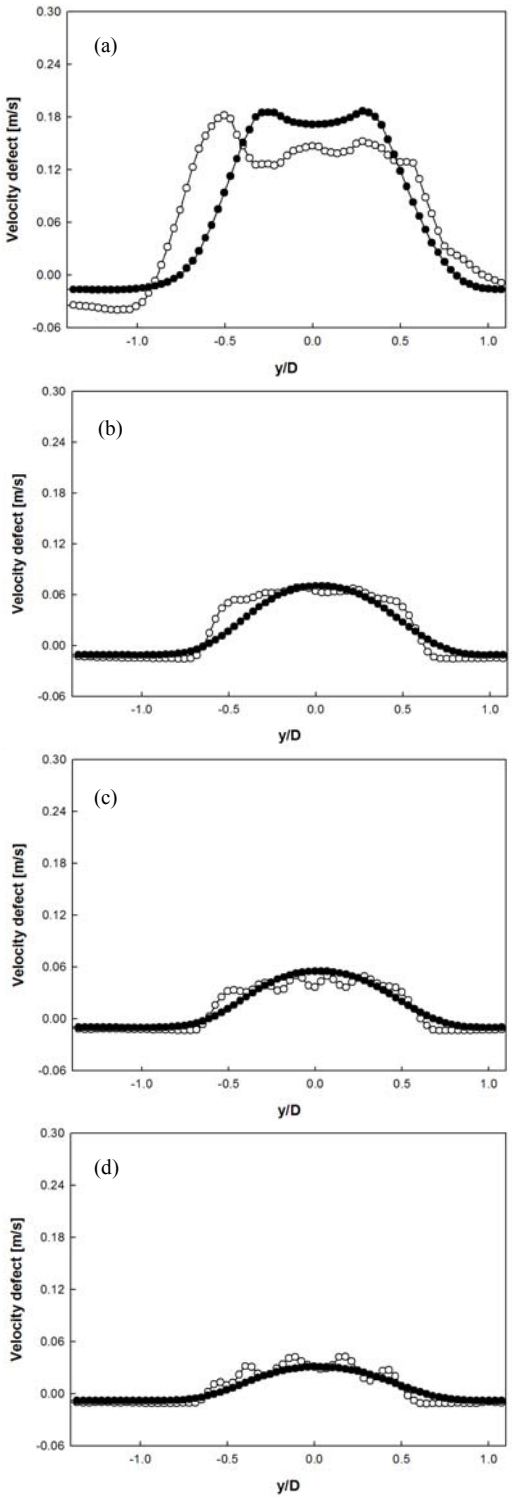

Fig.7. Velocity defect comparison with experiment and simulation in the wake of 1.5 diameter downstream from the centerline of the vertical cylinder at Re=20000. (a) 0% open cylinder; (b) 75% open cylinder; (c) 82% open cylinder; (d) 90% open cylinder. ○: experiment(Gansel et al.,2008) ●: simulation.

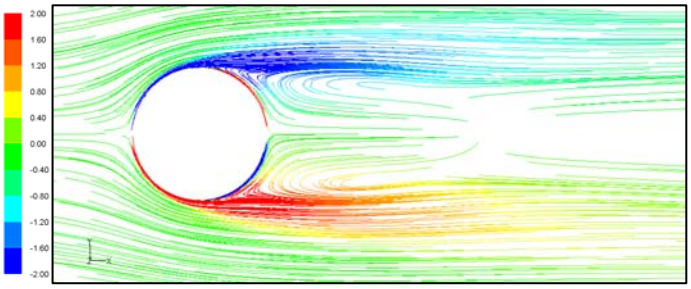

(a)

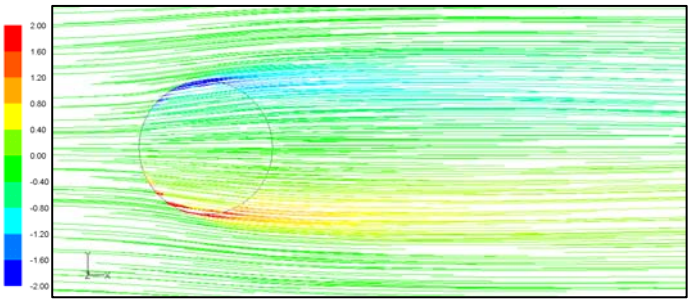

(b)

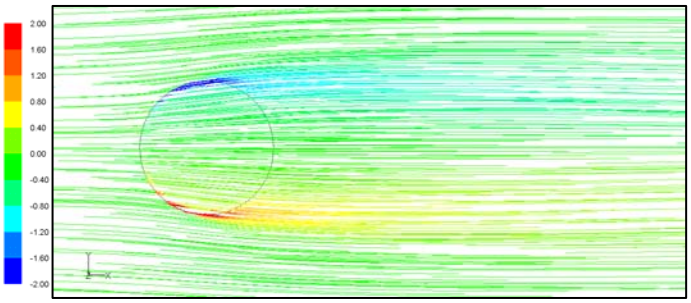

(c)

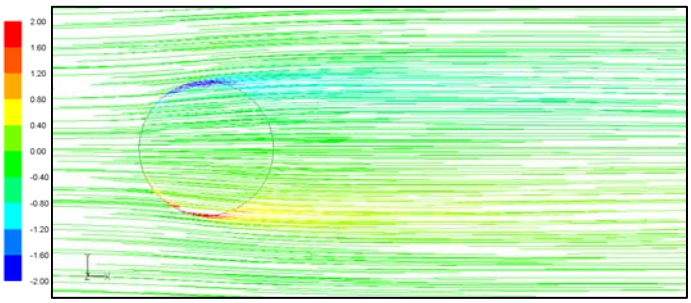

(d)

Fig.8. Streamlines for the flow through the cylinder rendered by contours of the vorticity in the z/D=1.5 at Re=5000 (a) 0% open cylinder; (b) 75% open cylinder; (c) 82% open cylinder; (d) 90% open cylinder.

both the external and internal flow fields. The porous cylinder partially diverts the flow. At the high porosity, the streamlines pass easily through the porous region. Meanwhile as the porosity decreases, the streamlines trend shift to the side of cylinder since porous interface deflect the upstream flow at the front area; therefore, the strength of vorticity is increased with the decrease of the porosity. Also, the length of the vorticity reduced as the porosity increases. The flow movement of the separation point downstream contributes to this phenomenon: this phenomenon has been studied by S. Bhattacharyya et al.(2006). With increasing open area the velocity of the fluid at the porous interface increases. This velocity has the effect of reducing the drag force. Hence a streamline for low open area cylinder flow into the porous interface which is leads to increased drag coefficient compare to the high open area cylinder.

CONCLUSIONS

A numerical study of the drag force and flow field in and around a porous cylinder has been applied with porous boundary condition for 5000 and 20000 Reynolds numbers. Numerical results were compared to experimental data previously published. The computed drag coefficient of the 0%, 75%, 82% and 90% open cylinder and sampling velocity defect are used for comparison with Gansel et al. 's (2008) results.

The computational model has been shown reasonable estimation of drag coefficient and velocity profile on a solid and porous cylinder for 5000 and 20000 Reynolds numbers. The drag coefficient measured on the porous cylinder shows that it is decreasing with increasing of the porosity due to the increase of permeability and decrease of pressure jump-coefficient.

ACKNOWLEDGMENTS

Authors are grateful to Lars Gansel for provision of experimental data and clarification of its use. This work has been financed by the Norwegian Research Council.

REFERENCES

[1] Igor Tsukrov., et al., 2003. "Finite element modeling of net panels using a consistent net element", Ocean Engineering (30) 251-270.

[2] Pa°l F. Lader, Arne Fredheim., 2006. "Dynamic properties of a flexible net sheet in waves and current-A numerical approach", Aquacultural Engineering (35) 228-238.

[3] Jochen Frohlich, Wolfgang Rodi., 2004, "LES of the flow around a circular cylinder of finite height", International Journal of Heat and Fluid Flow (25) 537-548.

[4] Taehun Lee, Ching Long Lin and Carl A. Friehe., 2007, "Large-eddy simulation of air flow around a wall-mounted circular cylinder and a tripod tower", Journal of Turbulence 8 (29).

[5] Kawamura, T., Hiwada, M., Hibino, T., Mabuchi, I., Kamuda, M., 1984. “Flow around a finite circular cylinder on a flat plate”, JSME 27 (232), 2142–2151.
[6] Okamoto, S., Sunabashiri, Y., 1992. “Vortex shedding from a circular cylinder of finite length placed on a ground plane”, J. Fluids Eng. 114, 512–521.
[7] S. Bhattacharyya, S. Dhinakaran and A. Khalili, 2006, “Fluid motion around and through a porous cylinder”, Chemical Engineering Science, 61, 4451–4461.
[8] Lars Gansel, Thomas A. McClimans, Dag Myrhaug., 2008, “effects of fish cages on ambient currents”, Proceedings of OMAE2008-57746
[9] Fluent. Fluent 6.3 User’s Guide. Fluent Inc. 2006-09-20